

Paleoneurology of an “early” Neandertal: endocranial size, shape, and features of Saccopastore 1

Emiliano Bruner*, Giorgio Manzi

Dipartimento di Biologia Animale e dell'Uomo, Università La Sapienza, Roma, Italia

Received 1 July 2005; accepted 10 August 2007

Abstract

The Saccopastore 1 cranium was found near Rome in 1929, and its most probable age is about 120 ka (OIS 5e). The Neandertal morphology of the specimen was recognized just after the discovery by the Italian anthropologist S. Sergi, and subsequently confirmed by several authors. The present paper provides a complete description and analysis of the endocranial shape and features of this specimen, considering anatomical traits, metrics, and landmark data. The main endocranial diameters and the vascular traces resemble the morphology displayed by Middle Pleistocene humans, although lacking some traits described in the European samples referred to as ante-Neandertals. Nevertheless, proportions and endocranial shape support a definite Neandertal morphology, mostly taking into account the lateral development of the frontal lobes and the shape of the parietal areas. Therefore, it may be hypothesized that the Neandertal neurocranial architecture was present since at least OIS 5, as already suggested on the basis of ectocranial morphology.

© 2007 Elsevier Ltd. All rights reserved.

Keywords: Paleoanthropology; Computed tomography; Endocast; Brain morphology

Introduction

Two fossil crania were discovered in a gravel quarry now within the city of Rome, Italy, in 1929 and 1935, respectively (Sergi, 1929; Breuil and Blanc, 1936). At that time, the site was enclosed within a rural area called Saccopastore, and the two specimens were named Saccopastore 1 and 2 (Fig. 1). Both came from alluvial sediments referred to the last interglacial period, possibly ranging between 130 and 100 ka; that is, toward the beginning of the oxygen isotopic stage (OIS) 5, and more probably OIS 5e (for details and references, see Bruner and Manzi, 2006).

The cranium known as Saccopastore 1 (SCP1) has been attributed to a mature female (Sergi, 1944). The skull is well-preserved, although it lacks the mandible and both the

zygomatic arches. Further damage was caused upon its discovery by the workmen of the quarry—the supraorbital region was heavily damaged, a few dental crowns were broken (and lost), two holes were produced in the frontoparietal portion of the vault. The endocranial cavity is still partially filled with stone matrix, and the cranial capacity was estimated to 1,174 ml. Saccopastore 2 is a less complete specimen from the same site, lacking the entire vault, part of the base, and the left frontoorbital areas. The cranium has been attributed to an adult male, and the cranial capacity was estimated between 1,280 and 1,300 ml (Sergi, 1948). The morphology of the two crania from Saccopastore is rather similar, showing apomorphies described in the European Würmian Neandertals together with features displayed by the European Middle Pleistocene humans (e.g., Stringer et al., 1984; Manzi and Passarello, 1991; Condemi, 1992; Arsuaga et al., 1997; Manzi, 2004; Bruner and Manzi, 2006). This “intermediate” phenotype—already evidenced by S. Sergi (1962)—appears consistent with the chronology of the specimens and fits a regional anagenetic perspective of human evolution, commonly

* Corresponding author. Centro Nacional de Investigación sobre la Evolución Humana (CENIEH), Avda. De la Paz, 28; 09004 Burgos, España.

E-mail address: emiliano.bruner@cenieh.es (E. Bruner).



Fig. 1. The fossil crania Saccopastore 1 (top) and Saccopastore 2 (bottom).

Materials and methods

The endocast of Saccopastore 1

Saccopastore 1 has been CT scanned according to procedures commonly employed for fossil specimens (e.g., Zollikofer et al., 1998; Recheis et al., 1999; Spoor et al., 2000). The scan was performed by sequential and contiguous 1-mm slices. The endocast was then reconstructed after the digital removal of the endocranial stone matrix with semi-automatic densitometric filters, according to the current imaging procedures applied in paleoneurology (Schoenemann et al., 2006). The endocranial cavity was isolated by closing the passages between the endocranial volumes and the outer space through a manual segmentation of the surfaces approaching the endocranial profile. These passages include anatomical structures connecting the brain with the ectocranial environment (foramina for nerves and vessels, foramen magnum, optic and olfactory tracts) as well as artificial fractures and other damage. The largest extrapolated surface is the area associated with the left frontal and right frontoparietal holes produced at the time of the discovery, which partially hamper the correct anatomical interpretation of the underlying endocranial traces. CT analysis and segmentation were done using Mimics 7.0.

A stereolithographic model of the endocast was created to convert the digital replica into a physical object (see Hjalgrim et al., 1995), and a hollowed acrylate model was prototyped through object-fine-layer technique, using polypox resin with a wall thickness of 3.0 mm. A metric comparison computed on 28 interlandmark distances and eight three-dimensional landmark coordinates (frontal poles, occipital poles, lateral maximum width, endobasion, endoververtex) showed no significant differences between the digital and the physical reproduction. Although the digital models include all the morphological information available, a physical replica can be useful to handle the object (allowing a more direct inspection of the anatomical relief) and to produce a more homogeneous sample (considering that most endocranial collections rely upon physical casts).

Endocranial features

Characters commonly used in paleoneurology [such as petalias, circumvolutions, venous sinuses, and middle meningeal vessels (e.g., Holloway, 1978; Falk, 1987; Grimaud-Hervé, 1997; Bruner, 2003a); see [Online Supplementary Material](#)] were scored on the endocranial surface using both the digital and physical replicas. The imprints of the middle meningeal artery were taken into particular consideration. As a consequence of the unclear nature of these vascular traces (see Falk, 1993), the term *middle meningeal vessels* is preferred here. These vessels leave direct traces on the endocranial surface because of the tight structural relationship between the layers of the dura and the inner table. This vascular system has a major role in metabolism and possibly in thermoregulation of the cortical volumes, but little information is available to describe and quantify the variability of this trait in extant and extinct human populations (Marcozzi, 1942; Falk and

referred to as the “accretion model” (e.g., Dean et al., 1998; Hublin, 2000).

A computed tomography (CT) based reconstruction of the two crania from Saccopastore was carried out to make the specimens available for digital surveys and analyses (Manzi et al., 2001), and the digital endocast of SCP1 was preliminarily reconstructed (Bruner et al., 2002). A quantitative analysis of the principal endocranial diameters showed that SCP1 is comparable to the Middle Pleistocene human variation in terms of absolute values, while the proportions relative to the maximum endocranial length suggest a more derived Neandertal morphology (Bruner et al., 2003a). A further quantitative assessment of the endocranial geometry corroborated the alleged phenotypic affinity between SCP1 and Neandertals, most of all because of the morphology of the parietal areas (Bruner, 2004).

Although this fossil has been commonly recognized as an early representative of the Neandertal lineage based on both ectocranial and endocranial morphology, a complete description of its endocranial anatomy and features has never been provided. In the present paper the endocast of SCP1 is described and discussed in detail, in order to provide a complete paleoneurological characterization of this specimen.

Nicholls, 1992; Falk, 1993; Grimaud-Hervé, 1997; Bruner et al., 2003b; Bruner et al., 2005). The pattern of the meningeal system is most commonly scored in terms of derivation of the middle (obelic) ramus from either the anterior (bregmatic) or the posterior (lambdatic) branches. These patterns are respectively referred to as Adachi's type I and type II, while the derivation of the obelic network from both the main branches is referred to as Adachi's type III (see Bruner et al., 2005, for further details).

Morphometrics

The physical endocast was analyzed by means of both traditional interlandmark distances and landmark-based superimposition, in order to provide a metrical description of the SCP1 endocranial morphology. A set of endocranial diameters was used for univariate and bivariate comparisons. Maximum hemispheric length (ML) was averaged between right and left hemispheres. The maximum endocranial width (MW) was taken orthogonally to the maximum length and to the mid-sagittal plane. The frontal width (FW) was measured at the most prominent areas between the opercular part (*pars opercularis*) and the triangular part (*pars triangularis*) of the third frontal circumvolutions, namely at the Broca's cap. Hemispheric length, endocranial width, and frontal width were measured with calipers. Anterior, middle, and posterior vault heights were measured as orthogonal projections at 0.25 (H1), 0.50 (H2), and 0.75 (H3), respectively, of the maximum hemispheric chord length. Heights were sampled as projections on the left hemisphere, using a dioptograph. Raw variables have been considered as well as relative variables, as the ratio between the values and the maximum hemispheric length (averaged hemispheres). Cranial capacities were collected from the literature (Grimaud-Hervé, 1997; Holloway et al., 2004). Metrics were computed using Statistica 5.1 (StatSoft, 1995) and PAST 1.56 (Hammer et al., 2001).

A landmark-based approach was used to provide a geometric description of the SCP1 endocranial general morphology. Although in geometric morphometrics superimpositions are often employed as a preliminary step to multivariate statistics, their raw application is nonetheless useful as a direct and simple morphological tool. When the paucity of the fossil record hampers a correct and balanced application of ordination techniques, paleontologists may rely upon very subjective and vague descriptions of specimens or traits. Geometric superimpositions provide a more objective approach to the morphological description, considering both the standardization of the procedures and the visualization tools available for these purposes (Bruner, 2006). Similarly, the deformation grids available using the thin-plate spline interpolant functions allow a synthetic visualization of the spatial differences, being independent of the superimposition criterion and providing a geometrical model for the whole surface (Bookstein, 1991).

Two-dimensional coordinates were sampled in left lateral view, using a dioptograph and a 12 landmark configuration (Fig. 2). Pairwise geometric comparisons were performed using the baseline registration and thin plate spline deformation grids (Bookstein, 1989, 1991). The baseline was computed using the frontal and occipital poles. This approach was considered useful to investigate shape differences with respect to a structural axis, here represented by the endocranial main diameter, approaching the hemispheric length. This superimposition can be rather informative considering the configuration used in this descriptive analysis, which largely depends upon these two reference points. Other registration procedures (like the Procrustes superimposition) are more suited in the multivariate context, in which the patterns of covariation are considered (see Zelditch et al., 2004, for a detailed discussion on these topics). It is also worth noting that in previous landmark-based comparisons endocranial geometry was largely described using anatomical references (for the vault profile, the presumed boundaries between frontal, parietal, and occipital lobes). In contrast, the current comparison is more strongly

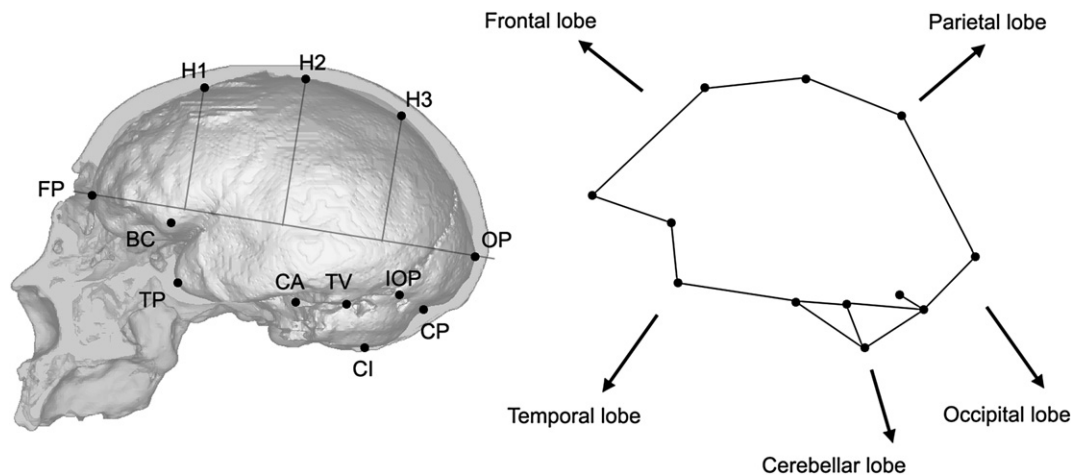


Fig. 2. Landmark configuration (left) and wireframe (right) used in the 2D pairwise analyses, shown on the digital endocast and sectioned digital replica of SCP1. BC: Broca's cap; CA: anterior edge of the cerebellum; CI: inferior edge of the cerebellum; CP: posterior edge of the cerebellum; FP: frontal pole; H1, H2, H3: endocranial height at 25%, 50%, and 75%, respectively, of the frontal-occipital baseline; IOP: internal occipital protuberance; OP: occipital pole; TP: temporal pole; TV: temporal valley (for further details, see Bruner, 2004).

based on geometrical references (for the vault profile, the height at given fractions of the frontooccipital chord), to rely on a more generalized descriptive approach. Superimpositions, average shapes, and pairwise comparisons were computed using Morphueus et al. (Slice, 2000).

Comparative endocasts were grouped according to their general taxonomic affinity, and average values were computed for each group. The Asian *Homo erectus* sample (HE) includes specimens from the Early and Middle Pleistocene of Java and China (Trinil 2, Sangiran 2, Zhoukoudian 3, 10, and 12). The Neandertal group (HN) includes Würmian Neandertals (La Chapelle aux Saints, La Ferrassie, Teshik Tash, Guattari, Feldhofer). The modern sample (HS) includes anatomically modern humans from late Pleistocene and early Holocene European sites (Predmosti 3, 4, 9, and 10, Combe Capelle, Vestonice 2, Vatte di Zambana). In addition, the endocast of the North African specimen from Salé (Middle Pleistocene, Morocco) was considered, in view of its hypothesized lack of derived endocranial traits (Bruner, 2003b, 2004). The endocasts were sampled at the Museum of Anthropology of the University La Sapienza, Roma, at the Istituto Italiano di Paleontologia Umana, Roma, and at the Institut de Paléontologie Humaine, Paris.

Results

General morphology and discrete features

The attenuation spectrum of SCP1 shows a bimodal distribution, characterized by two partially distinct phases. A first peak represents the lower density component ($2,768 \pm 252$ Hounsfield units, Hu), which includes most of the fossil matrix, except the dental enamel and cementum. The lower and higher halves of this curve represent outer and inner layers of the fossil volume, respectively. A second peak ($3,623 \pm 178$ Hu) represents the higher density phase and is mainly composed of the stone matrix, including that on bone surfaces (e.g., endocranial cavity, petrous pyramids, and sinuses) and that within bone (e.g., frontal and occipital diploë). A very low component ($1,894 \pm 186$ Hu) includes light geological infiltration and a large inclusion in the right maxillary sinus, plus some partial volume effect (see Spoor et al., 2000). Considering the fossil matrix, the vault is totally defined by the first phase, whereas the two components are blended in the facial structures, with the second phase distribution increasing downward. Both phases are distinguishable, but a certain degree of superimposition makes a complete separation impossible. A metric ectocranial comparison between the fossil and its digital replica shows an average difference of 0.55 mm, close to the voxel resolution ($0.49 \times 0.49 \times 1.00 \text{ mm}^3$). Some difficulties may be found in the exact landmark localization, because of the triangle-based 3D reconstruction that produces irregular surfaces with discrete units at high magnification. With a selection of highly visible landmarks the average difference falls to 0.33 mm.

The endocranial cavity is partially filled by a homogeneous inclusion that can be digitally removed with automatic and semi-automatic procedures. It reproduces an accurate

“natural” cast including the cerebellar and occipital poles of both sides, the right temporal lobe, and the proximal component of the right 3rd frontal circumvolution. The endocast can be segmented almost entirely, reproducing both the general morphology and several details (Fig. 3). Only the basal structures (clivus and temporal bases, including the temporal pyramids) cannot be entirely modelled due to the intimate densitometric overlap in these areas. Two different cranial capacity estimations based on voxel count give comparable values, averaging 1,094 ml.

The left frontal lobe only slightly exceeds the right one anteriorly, while in contrast the right lobe is wider (Fig. 4a). Conversely, the occipital poles show a marked left dominance in length and width (see Fig. 3). The proximal tract of the third frontal circumvolutions is more delineated on the left hemisphere. Also, the supramarginal gyrus is more visible on the left hemisphere, while the counterpart is smoother but more expanded. The Sylvian fissure cannot be clearly identified, while the Rolandic and perpendicular ones show some weak but visible traces. The maximum width is localized at the base of the 3rd temporal circumvolution in the left hemisphere, while in the right one it is shifted upward, at the level of the temporoparietal boundary. On this side, the coronal profile is smoother and more gradually convex. Nevertheless, the posterior view shows a clear *en bombe* profile, when both sides are considered. The lateral view shows a regular and continuous upper midsagittal outline, with only a slight depression close to the parietooccipital boundary, but without projecting occipital poles.

The encephalic rostrum is clearly shaped, and details of frontal gyri and sulci are easily recognizable. Some scattered surfaces around these areas represent residual geological encrustations. Although the orbital torus is largely missing, the orbital lobes appear localized almost entirely on the orbital roof, rather than behind it (Fig. 4b). The three principal orbital circumvolutions are more clearly visible on the left hemisphere. The frontal sinuses, almost entirely visible on the ectocranium because of the browridge damage, do not expand within the frontal squama.

The crista galli is completely preserved, large, and pneumatized, but not clubbed (Fig. 5). It is in an anterior and superior position with respect to the nasal pit, and not directly placed on the floor of the anterior fossa at the center of the cribriform plate. Furthermore, it is rather posteriorly tilted, with the posterior edge oriented vertically and the base attached almost on the frontal wall. The pneumatization is continuous with the network of the ethmoidal air cells. The medial margin of the orbital roof is clearly visible, but not very sharp or vertical. The cribriform plate is opened, and not flattened between the medial orbital margins. The entire area is included within the depression of the encephalic rostrum, where the medial third of the orbital roof is smoothly inclined to form this small medial fossa. The thickness of the orbital roof (averaged from 32 available different points) measures 2.9 ± 0.5 mm. The frontal crest is sharp and robust. The right clinoid process is extremely enlarged, shifting the entire morphology of the frontal base. The left clinoid process is much smaller, probably

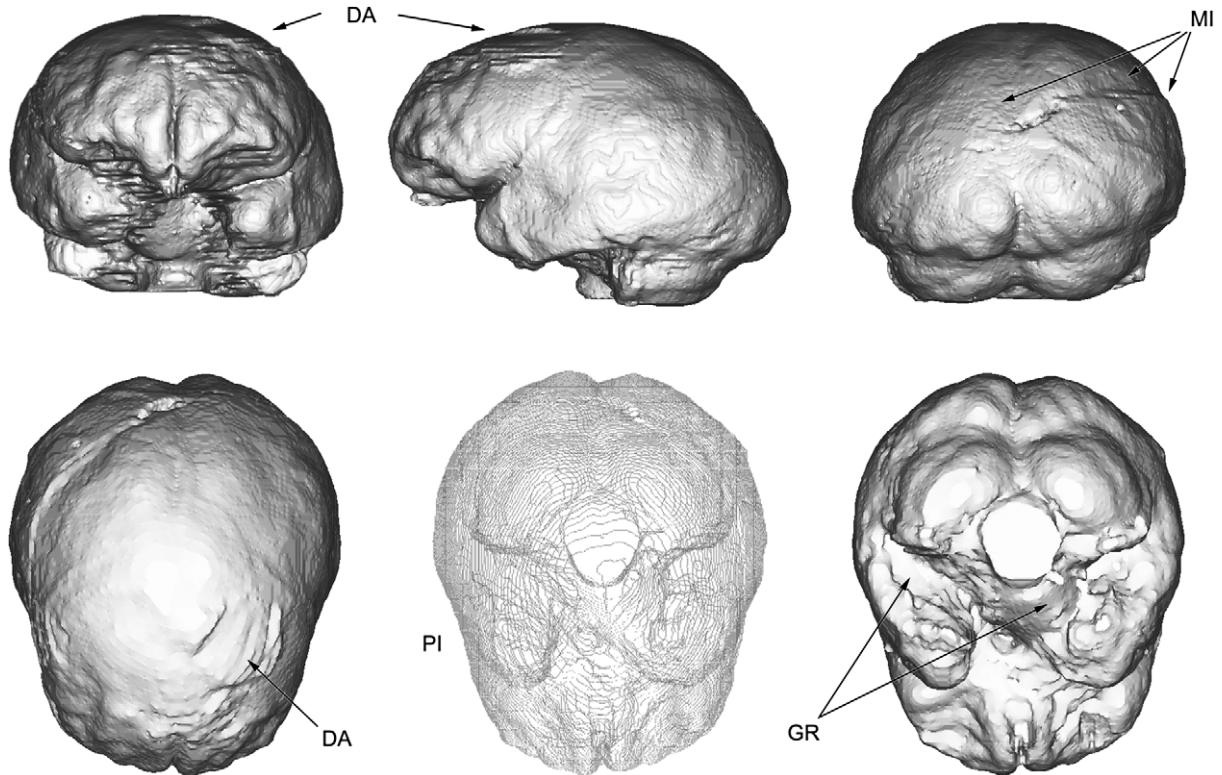


Fig. 3. Digital replica of the SCP1 endocranial cavity. PI: polylines interpolation; DA: damaged areas; GR: geological residuals; MI: interface between matrices (i.e., sediment-filled and empty volumes of the endocranial cavity).

forming a carotid-clinoid bridge. Overall, the area of the sella is heavily obscured by the geological matrix. Accordingly, it is rather difficult to assess the actual morphology of these structures.

The parietal areas do not show any relevant circumvolution, except for the supramarginal relief on the left side. The occipital lobes are somewhat flattened against the parietal ones, without a marked occipital projection or flexion of the

midsagittal outline. The cerebellar lobes are mainly positioned under the parietal area. Their shape is rather globular and slightly lengthened. Their principal axes are oblique to the midsagittal plane with an angle of approximately 45° each (left 45° , right 39°). Thus, the two axes approach a 90° angle. The cerebellar lobes are placed behind and laterally with respect to the brainstem, nearly touching one another

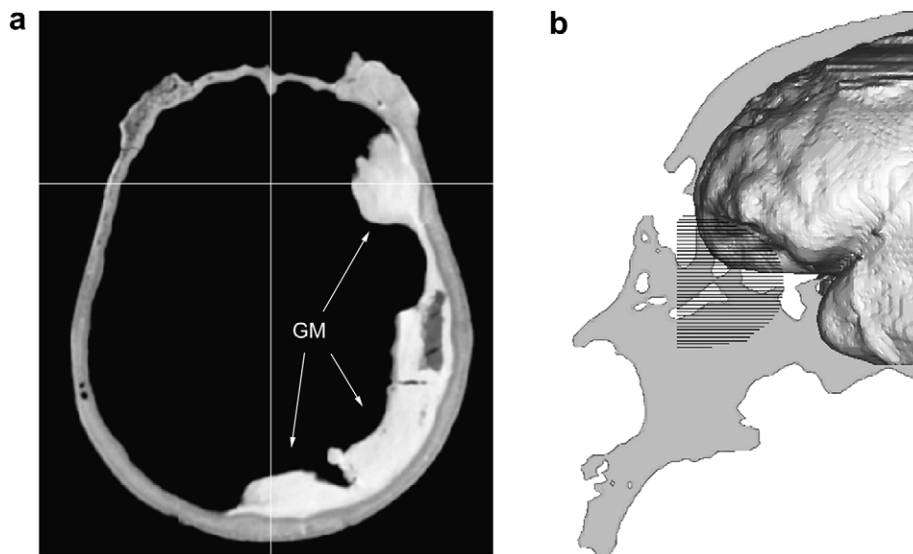


Fig. 4. a) The transversal tomographic section shows the frontal area in SCP1 displaying only minor asymmetries, with the left lobe slightly longer and the right one wider. GM: geological matrix included within the endocranial cavity. b) A digital reconstruction of the endocranial cavity in left lateral view is represented with the midsagittal section of the skull (grey profile) and the medial outline of the left orbit (shaded), showing the frontal lobes localized approximately upon the orbital roof.

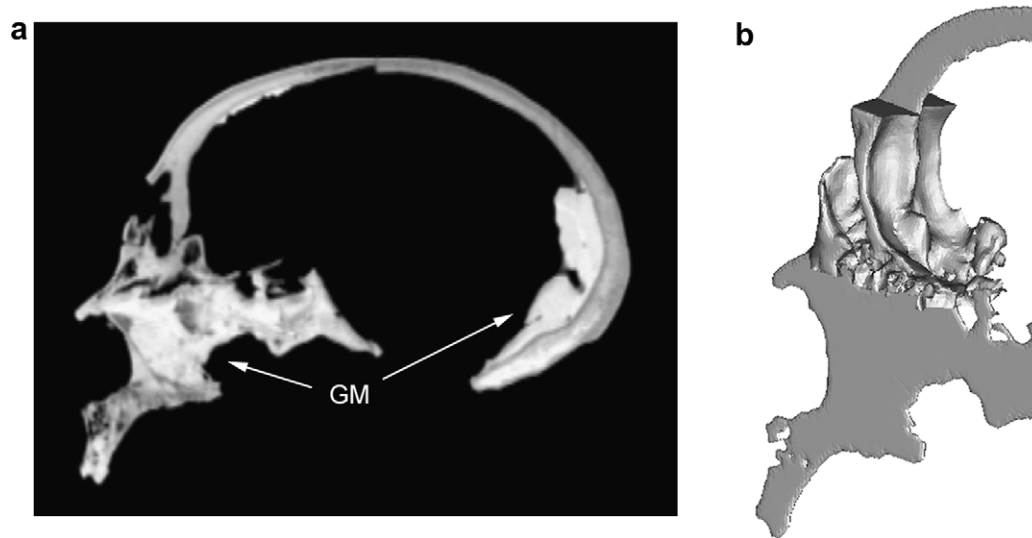


Fig. 5. The crista galli of SCP1 is large and pneumatized, localized anteriorly to the cribriform plate contacting the frontal wall of the anterior fossa, and rather tilted backward: (a) midsagittal section of the skull and (b) digital reconstruction of the medial volumes of the anterior fossa. GM: geological matrix.

posteriorly. The superior sagittal sinus is only clearly visible between the parietal lobes and at the confluence of the sinuses, where it turns into a well-developed and enlarged right transverse-sigmoid system. The sagittal sinus runs into the right transverse sinus almost from the upper portion of the occipital poles, without crossing the internal occipital protuberance. The left transverse-sigmoid system is barely localizable, but still visible. A defined prominence, anterior and superior to the right sigmoid sinus, can be interpreted as a temporal arachnoidal granulation. No occipitomarginal system is detected.

The pattern of the middle meningeal vessels is partially visible on both hemispheres (Fig. 6a). The right meningeal system shows a single anterior branch that starts from the foramen spinosum and approaches the Sylvian valley. The trace crosses the temporal pole and fades above into a damaged zone. The posterior ramus includes a long and single lambdatic branch and a developed obelic derivation. The latter appears branched at least once; its major segment reaches the supramarginal gyrus, while a smaller trace runs parallel to the lambdatic branch up to the angular gyrus. The trace of

the left meningeal vessels is similar to the pattern described for the right hemisphere (Fig. 6b). It shows a long and scarcely arborized anterior ramus, with the posterior one including both the lambdatic and obelic branches. These two vessels are both bifurcated but scarcely developed, and their traces (mostly the middle branches) are rather feeble. Thus, the middle meningeal pattern of SCP1 (both sides) may be referred to the Adachi's type II pattern, with dominance of the posterior double-branched vascular system. No anastomoses were detected. The hypothesized arachnoidal granulation (see above) is located beneath the right lambdatic ramus, at the base of the temporal lobe.

Morphometrics

In Table 1, the mean values of interlandmark distances and other dimensions are reported for the three comparative groups (HE, HN, and HS), and compared with Salé and SCP1.

The SCP1 cranial capacity is intermediate between the Asian *Homo erectus* (HE) and the other (European) groups.

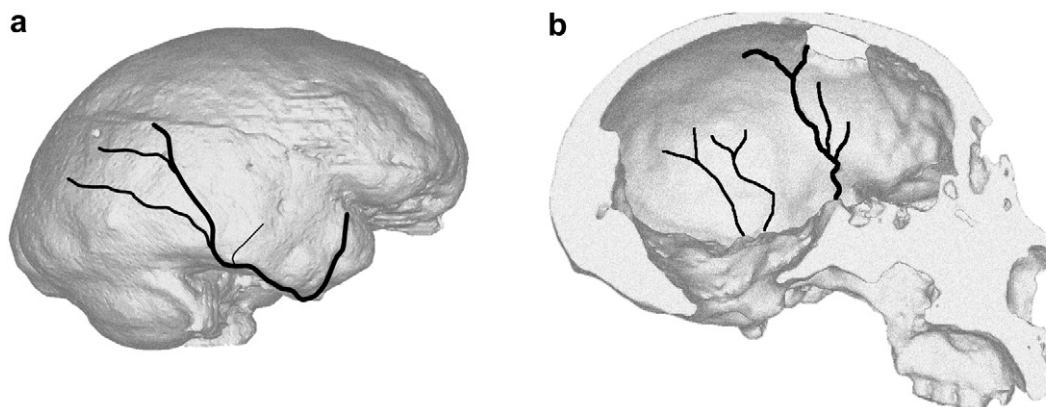


Fig. 6. Endocranial traces of the middle meningeal vessels in SCP1's right (a) and left (b) hemispheres (note: drawings are not to the same scale).

Table 1

Mean values for Asian *Homo erectus* (HE), Neandertals (HN), and anatomically modern humans (HS), compared with the values from Salé and SCP1. HL: hemispheric length; MW: maximum endocranial width; FW: frontal width; H1, H2, H3: anterior, middle, and posterior vault heights; CC: cranial capacity. Measurements in mm, except capacity. See text for definition

	Absolute values							Relative values				
	HL	MW	FW	H1	H2	H3	CC	MW	FW	H1	H2	H3
HE	160	125	94	49	59	50	991	0.78	0.58	0.30	0.36	0.31
HN	178	142	112	58	71	59	1567	0.80	0.63	0.33	0.40	0.33
HS	183	139	111	66	80	72	1525	0.76	0.61	0.36	0.44	0.39
Salé	149	116	85	50	59	52	880	0.78	0.57	0.33	0.39	0.34
SCP1	161	131	102	51	61	53	1174	0.82	0.64	0.31	0.37	0.33

The result is similar whether using the estimate proposed by Sergi (1,174 cc) or the value computed by a voxel count of the digital replica (1,094 cc).

With respect to the main endocranial diameters, the hemispheric length and the vault heights are similar to the HE mean, the latter two being also very close to the Salé metrics. In contrast, the endocranial widths show intermediate values between the less and more encephalized groups. When adjusted to endocranial length, vault height is comparable to the average nonmodern groups, while the endocranial widths are similar to the Neandertal mean values. Clustering these values using the unweighted pair-group method using arithmetic averages (UPGMA), SCP1 shows an overall metric similarity with the mean HE figure and Salé when the raw metrics are considered, but groups with HN average values when using the hemispheric-adjusted metrics (Fig. 7). When the metrics adjusted for endocranial length are used to perform a principal component analysis, the first component (75% of the variance) is associated with the frontoparietal height (most of all, the posterior diameter), and the second (17%) to the endocranial widths (mostly the frontal diameter). The three groups are rather separated using these two axes, and SCP1 is definitely included in the Neandertal range (Fig. 7c).

Considering the relationship between endocranial length and endocranial widths, only Guattari 1 stands outside the 95% confidence intervals of the present sample, because of its large frontal diameter (Fig. 8a,b). SCP1 shows large endocranial widths when compared with those specimens displaying a similar endocranial length (i.e., large-brained *Homo erectus*), most of all with respect to its frontal width. When the relationship between the frontal and maximum endocranial width are taken into account, SCP1 is intermediate between the less encephalized (*Homo erectus* and Salé) and more encephalized (Neandertals and modern humans) specimens (Fig. 8c) along the allometric trajectory. When the ratio between frontal and maximum endocranial width are considered, the morphology from Salé stands within the *Homo erectus* variation, while the morphology of SCP1 stands within the Neandertal standard error (Fig. 8d).

When the middle vault height is regressed on endocranial length, SCP1 fits the expected value of endocranial vertical development, whether considering the whole sample or just the nonmodern specimens (Fig. 9).

Taken together, these simple endocranial dimensions suggest that the endocast of SCP1 shows a frontoparietal vertical

development expected for its brain length, but has the endocranial width (and, consequently, the lateral brain enlargement) displayed by Neandertals.

The landmark superimposition and thin-plate spline distortion grids allow for further considerations of the lateral endocranial profile, comparing the configuration of SCP1 with that of Salé, and with the average shapes of the other comparative samples.

Salé vs. SCP1 (Fig. 10). Compared in terms of the same hemispheric length in lateral view, SCP1 shows a flatter vault, and cerebellar hemispheres in a more anterior position. The grids also stress a dilation of the temporoccipital structures, mostly at the lower areas. The overall shape is rather similar, except for the inferoposterior warp associated with relative enlargement and anterior shifting of the cerebellar structures.

HE vs. SCP1 (Fig. 11). Unfortunately, the Asian specimens lack the cerebellar structures; thus, the superimposition was performed on the remaining landmarks. Nevertheless, the result appears similar to the previous comparison. The vault in SCP1 is only slightly higher than the *Homo erectus* representatives, the cerebellar lobes are more anterior (at least considering the posterior edges), and the lower temporoccipital areas are expanded vertically. In contrast, the lower half of the occipital lobes is more developed posteriorly in the Asian group, with a relative deepening of the inner occipital protuberance. The grids emphasize the enlargement of the posterior lower areas, and the posterior flattening of the occipitocerebellar volumes.

HN vs. SCP1 (Fig. 12). This comparison shows only limited deformation compared with the previous two (see below), reflecting a certain phenetic affinity between SCP1 and the Neandertal consensus values. The vault of SCP1 is flatter than the Neandertal mean, but nevertheless within the range of variation of the group. The largest differences can be seen in the lower half on the endocast, which is rather short in its dorsoventral extension. The frontal, temporal, and cerebellar structures are vertically flattened, and the grids stress the corresponding compression of the clivus.

Excluding the cerebellar landmarks, the Procrustes distance from SCP1 to the other configurations was 0.057 (Salé), 0.072 (HE), and 0.042 (HN), respectively. Similarly, using the thin-plate spline interpolant function the bending energy to warp the SCP1 configuration into the others was 0.039 (Salé), 0.114 (HE), and 0.025 (HN), respectively. That is, SCP1 is quantitatively more similar to the mean Neandertal shape, taking into

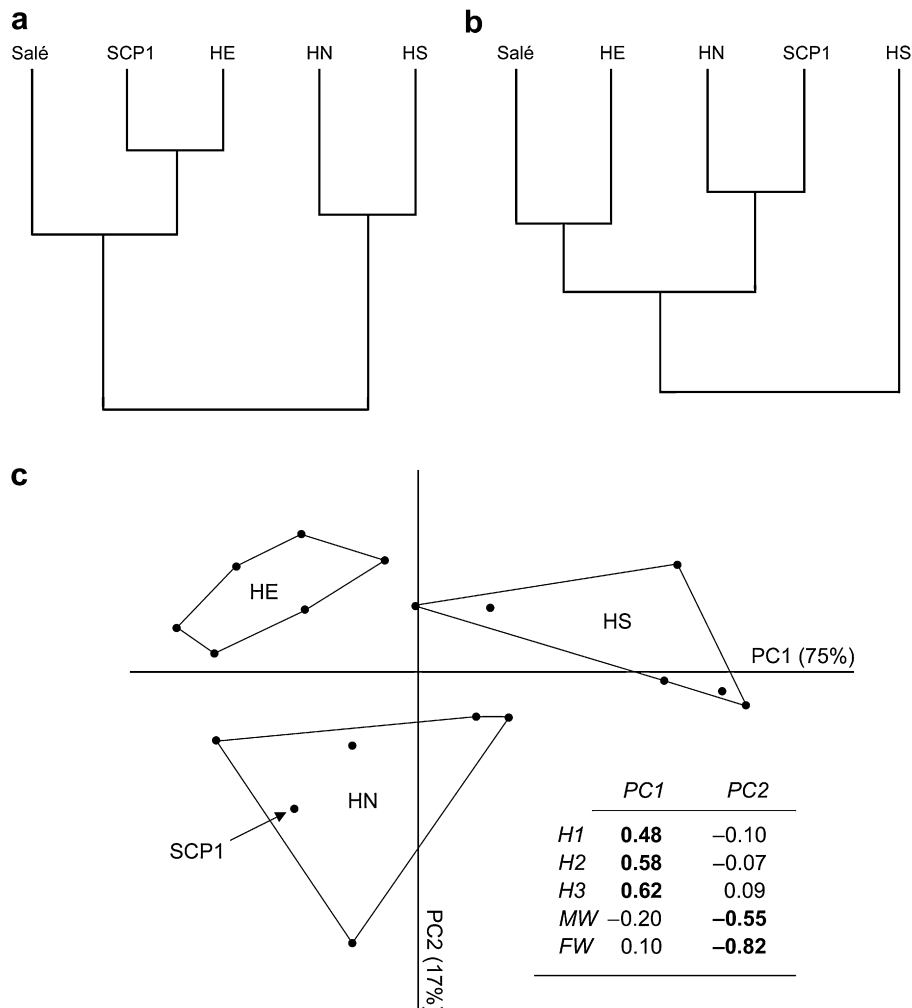


Fig. 7. Phenetic affinity between SCP1, Salé, and the average values of *Homo erectus* (HE), Neandertals (HN), and modern humans (HS), using the raw (a) and adjusted (b) metrics. Cophenetic correlation coefficients are 0.83 and 0.87, respectively. A principal component analysis on the adjusted metrics (c) separates the three groups according to the frontoparietal heights (PC1) and endocranial widths (PC2). SCP1 (arrow) is included within the Neandertal range. Convex hulls and the table of the loadings are also shown. H1, H2, H3: anterior, middle, and posterior endocranial vault heights, respectively; MW: maximum width; FW: frontal width; determinant loadings in bold.

account both the overall geometric differences (Procrustes distances) or the localized nonaffine changes (bending energy).

Discussion

Saccopastore 1 represents an interesting opportunity to test the interaction between phylogenetic and structural (allometric) signals within the functional matrix of the skull, in the general framework of the evolution of the genus *Homo*. Although this specimen has been commonly referred to the Neandertal lineage (pre-Neandertal or “early” Neandertal; Sergi, 1962; Condemi, 1992; Dean et al., 1998) the overall size is smaller than the Würmian populations. Because of the comparative data already published elsewhere on Neandertal endocranial variation, and because of the limited statistical power often associated with the scanty fossil samples, we have provided a complete descriptive report on the SCP1 endocranial morphology here, rather than a quantitative assessment of the phenotypic patterns of variation.

The digital endocast reconstructed using computed tomography provides a cranial capacity that is 80 cc lower than the original morphometric estimate put forth by Sergi (1,174 mL; Sergi, 1944). The digital approach is likely to be more precise than a mathematical model based on traditional metrics. Nevertheless, it must be noted that our digital replica of the endocast lacks small volumes of the lower temporal areas and that the clivus obscured by the geological infiltrations, possibly accounting for a portion of the observed discordance. However, because the results presented here do not change regardless of which proposed value is adopted, this minor difference will not be discussed further.

Some characters described in the SCP1 endocast are probably shared among all the extinct and extant human groups. The petalias displayed by this specimen (right frontal, left occipital) are within the range of human variation, and (although rarely expressed in combination) also exist in living great apes (Le May, 1976; Holloway and De La Costelareymondie, 1982). The function and consequences of different patterns

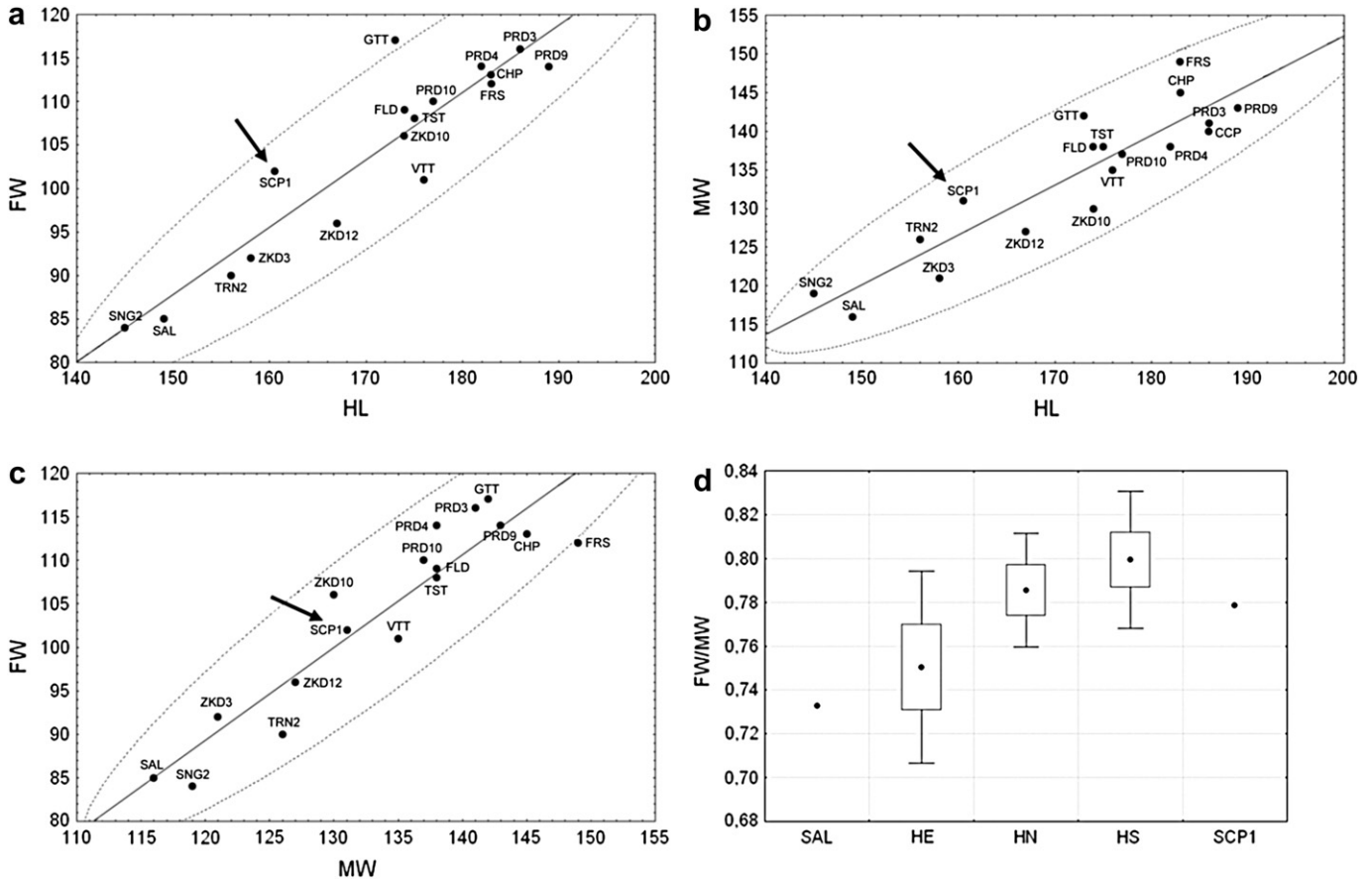


Fig. 8. Endocranial widths: frontal (a) and maximum (b) widths (FW, MW) are regressed onto hemispheric length (HL) and reciprocally correlated (c). Dotted lines show 95% confidence interval, solid lines show the least-square fit; values are in mm. (d) The ratio between frontal and maximum width is reported through box and whiskers showing mean, standard error, and standard deviations for each specimen or group; abbreviations as in Fig. 7. CCP: Combe Capelle; CHP: La Chapelle-aux-Saints; FLD: Feldhofer; FRS: La Ferrassie; GTT: Guattari; PRD: Predmost; SAL: Salé; SNG: Sangiran; TRN: Trinil; TST: Teshik Tash; VTT: Vatte di Zambana; ZKD: Zhoukoudian. The arrows point at SCP1.

of petalias is widely debated (see Bradshaw, 1988; Hellige, 1993). Although some relationships have been found between asymmetries and functions (e.g., Galaburda et al., 1978), there is no agreement on this issue. In SCP1 the frontal petalia is not so marked, and it mainly concerns the coronal development of the right side and the longitudinal extension of the left lobe. In contrast, the parietooccipital asymmetry is clearly apparent. The dominance of the left posterior areas with respect to the right ones involves a larger pressure on the endocranial surface on the left side, or a tighter contact between the layers of the dura mater and the bone. As a biomechanical response, it can be hypothesized that the blood outflow would be directed mainly through the contralateral transverse-sigmoid system, which would enlarge as a result. This relationship illustrates the possibility of correlating some *in vivo* physiological processes to observable postmortem anatomical details. Such an approach can be extremely useful when petalias cannot be directly assessed because of the fragmentary nature of the specimen. In SCP1 both features (left occipital dominance and enlarged right transverse-sigmoid system) are well expressed. The trace at the confluence of the sinuses is very clear, and it may be hypothesized that the left transverse sinus was isolated

from the right one and directly connected to the deeper straight sinus.

Another trait that falls within the range of extinct hominin variation is the low vault, when the brain length is taken into account. SCP1 has always been recognized as one of the most platycephalic Neandertals (Sergi, 1929, 1944), with a basion-bregma distance of 109 mm, included in the range of variation of less derived taxa such as *Homo erectus* (e.g., Rightmire, 1990). Also, a preliminary analysis of Saccopastore 1's digital endocast suggested a certain similarity with the low-vaulted Asian *Homo erectus* (Bruner et al., 2002). However, according to the available data, SCP1 displays an endocranial vault elevation expected for any nonmodern specimen with its hemispheric length. In this respect, the low vault is simply associated with the smaller brain size, when compared to the more encephalized classic Neandertals.

The comparison between SCP1 and Asian *Homo erectus* shows both differences and similarities. The overall endocranial dimensions are comparable, suggesting a similar degree of encephalization (in terms of brain volume). Also, the traces of the middle meningeal vessels are very similar, with a dominance of the posterior vascular channels, limited network, and no anastomoses (Grimaud-Hervé, 1997). Of course, it must be remarked

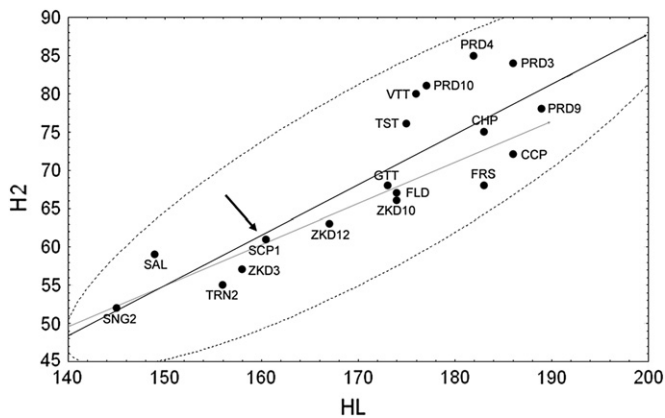


Fig. 9. Vault middle height (H2) is plotted onto hemispheric length (HL). Dotted lines show 95% confidence interval, solid lines show the least-squares fit. Grey line shows the least-squares fit for the nonmodern variation. Values are in mm, labels as in Figs. 7 and 8. The arrow points at SCP1.

that there is no full correspondence between the original soft tissues and the traces left on the endocranial surface. Some original vessels may have left their respective traces and other may not, depending upon parameters such as the endocranial pressure or the organization of the cortical mass (see Kimbel, 1984; O’Laughlin, 1996). In other words, the observed traces report the evidence of actual vessels, but we cannot exclude the presence of other structures that have not left any sign on the endocast. Furthermore, the prevalence of each pattern is quite heterogeneous, even among individuals of the same population (Marcozzi, 1942; Grimaud-Hervé, 1997; Bruner et al., 2003b), and a common scoring method of such traits does not exist. This feature was proposed to be useful for phylogenetic inferences mainly because of the increasing complexity of the middle meningeal network in modern humans (see Saban, 1995). These vascular systems should be analyzed in greater detail, considering the relationship between the middle meningeal vessels and the endocranial anatomy in terms of structural network and functional craniology, genetics, and phylogeny or, alternatively, neurofunctional system and cognition. Actually,

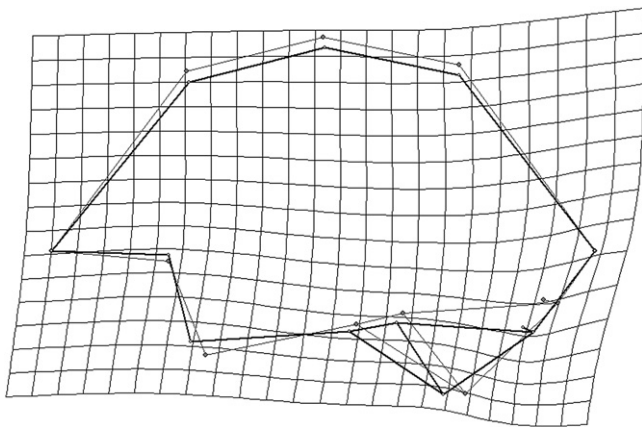


Fig. 10. The configuration of SCP1 (target, bold links) is superimposed on the configuration of Salé (reference, thin links) through the frontooccipital base-line, and the differences are visualized by using the thin-plate-spline distortion grids.

more complex traces can be described only for *Homo sapiens*, resulting either from increased vascularization or increased cortical pressure, with a consequent increase in the number of resulting imprints (Bruner et al., 2005). Previous studies have shown that the middle meningeal pattern of SCP1 is closely comparable to that of Krapina 3 (Bruner et al., 2006). Considering the overall resemblance between these two penecontemporaneous crania, we tentatively suggest this pattern as representative for the European pre-Würmian populations, and (whether a structural relationship between meningeal vessels and endocranial shape may be hypothesized) propose a comparable general endocranial morphology between the two specimens. Nonetheless, other Krapina parietal fragments support the hypothesis of a more variable phenotype, stressing the lack of knowledge about extinct (and extant) variability. The developed network of Krapina 21, together with a similar condition described for specimens like Arago (Grimaud-Hervé, 1997) and Biache (Saban, 1979), suggests that the presence of a parietal complex reticulation might not represent a unique modern human feature (e.g., Saban, 1982).

Because the above similarities between SCP1 and Asian *Homo erectus* may result simply from comparable brain size, the differences are perhaps more noteworthy. SCP1 lacks the occipital projection described for the Asian specimens (Bruner, 2004; Wu et al., 2006), and again evidenced in the present study. It is worth noting that the occipital morphology described for the Asian *Homo erectus* is not displayed by Salé (for a different view, see Holloway et al., 2004), and it is probably absent even in the Nariokotome endocast (Begun and Walker, 1993). It must be hypothesized that the occipital projection in the Asian group can be structurally associated with the posterior displacement of their cerebellar lobes. The shape comparison in lateral view also suggests that one of the major differences between SCP1 and more archaic forms can be detected at the lower temporooccipital area, which is expanded in the former. Whether this difference is related to a relative enlargement of those areas or to a structural pressure exerted by the parietal areas onto the lower districts still has to be determined. Finally, it is worth noting that, compared with other Middle Pleistocene morphotypes, SCP1 also lacks some traits described in the European endocasts, like frontal sinuses expanded within the frontal squama or the frontal lobes positioned behind the orbital roof (Seidler et al., 1997).

In contrast, the endocranial affinities between SCP1 and the other Neandertals are quite strong. The endocranial metrics, adjusted for endocranial length, support a Neandertal phenetic affinity regardless of whether single specimens (Bruner et al., 2003a) or group averages (this work) are considered. The ordination analysis performed on this small but simple set of hemispheric-adjusted endocranial main diameters synthesizes the principal characters of the groups considered, and it clearly supports the general Neandertal morphology of the SCP1 endocast.

The maximum endocranial width is localized at the temporal lobes in archaic morphotypes, and at the parietotemporal level among the Neandertals (Holloway, 1980, 1981; Grimaud-Hervé, 1997). In SCP1, the maximum width of the endocranium shows the same asymmetry detected in the skull,

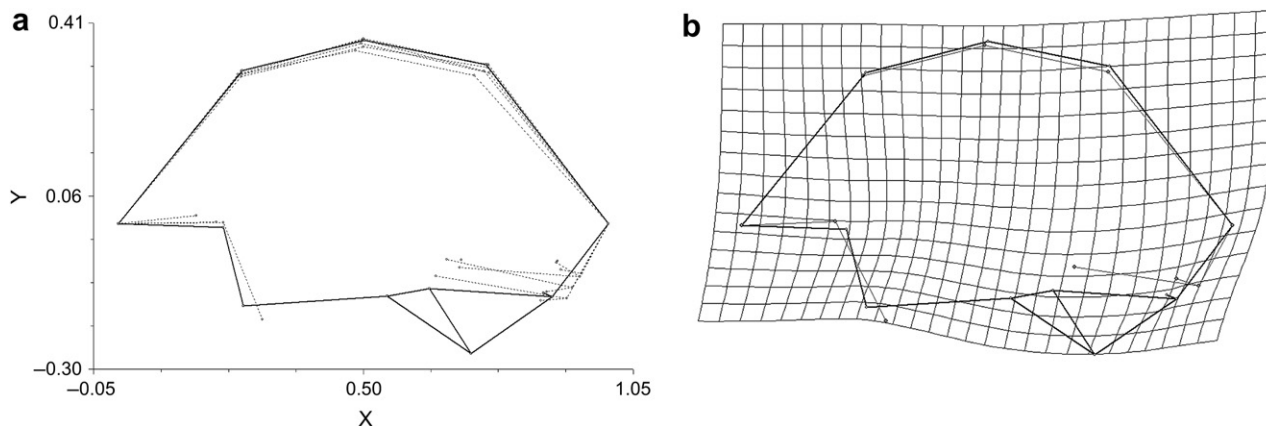


Fig. 11. The configuration of SCP1 (bold links) is superimposed on the configurations of the *Homo erectus* group (dotted links) through (a) the frontooccipital baseline, and (b) on their average shape used as reference (thin links).

where the right euryon is higher and more anterior than the left one (Sergi, 1944). Regardless, on both sides the maximum width is superior to the temporal areas, and the parietal surface of SCP1 clearly displays a Neandertal morphology. This is particularly clear when considering the widening of the upper parietal volumes and the consequent *en bombe* profile in posterior view (Bruner et al., 2003a).

Apart from the relative position of the maximum endocranial width, one of the most interesting observations concerns the lateral development of the brain. SCP1's endocranial is wide, especially at the Broca's cap. Although the values fall within the 95% confidence interval of *Homo* variation, it is definitely large when compared with endocranial showing the same endocranial length (that is, compared to *Homo erectus*). Also, the frontal lobes are wide when compared with the maximum endocranial width, approaching the ratio displayed by Neandertals and modern humans. In general, small-brained hominids show a visible coronal narrowing of the frontal lobes (Grimaud-Hervé, 1997). By contrast, among Neandertals and modern humans there is a general enlargement of the brain characterized by a more marked widening at the frontal lobes, which leads to

a more “squared” appearance in dorsal view. The frontal lobes were hypothesized to show a positive allometric widening with respect to the endocranial width along the encephalization trajectories because of spatial lateral availability and vertical structural constraints (Bruner, 2004). Whether or not this pattern fits a shared allometric trend within *Homo*, or whether Neandertals and modern humans depart from a more archaic morphology because of a functional and specific adaptation, remains to be tested using a larger sample. Regardless, the frontal widening of SCP1, together with the relative frontal narrowing described for the skull from Ceprano (Bruner and Manzi, 2005), may suggest a phylogenetic (nonallometric) relevance for this trait, considering the similar cranial capacity but the different evolutionary contexts for the two specimens.

Neandertals and ante-Neandertals have been described as having a high frequency of the trace of the sphenoparietal sinus (Gracia, 1991; Grimaud-Hervé, 1997), which may be considered as an interesting structural marker. The presence of this trait in SCP1 was hypothesized on the basis of an earlier reconstruction of the digital endocranial (Bruner et al., 2002). The present digital reconstruction does not clearly support the

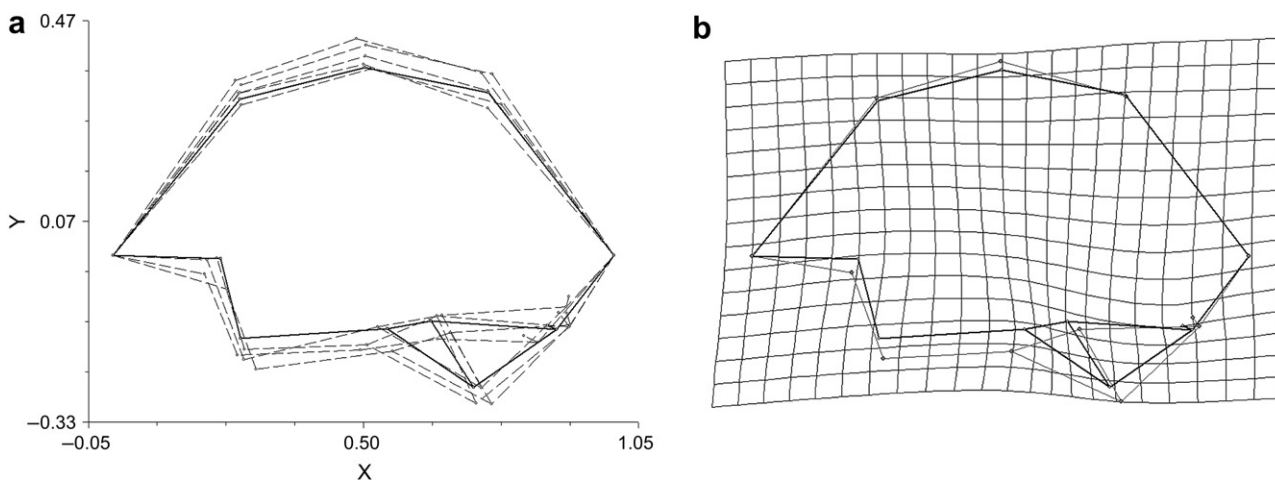


Fig. 12. The configuration of SCP1 (bold links) is superimposed on the configurations of the Neandertal group (dashed links) through the (a) frontooccipital baseline, and (b) on their average shape used as reference (thin links).

presence of an enlarged sphenoparietal sinus on SCP1's left hemisphere, since the observed trace has to be more properly interpreted as the imprint of the left middle meningeal vessels. However, it is important to note that the prevalence and expression of this feature is quite heterogeneous and difficult to assess (Bruner et al., 2003b), and a prevalence-based epigenetic character cannot be strictly interpreted as an autapomorphy because of its discontinuous presence within and among populations.

Finally, SCP1 shows some interesting endocranial traits that cannot be presently assessed in terms of evolutionary or phylogenetic relationships due to the lack of comparative data. The crista galli is large and tilted posteriorly. In general, the morphology of the crista is associated with the tension caused by the falx cerebri (Moss and Young, 1960). In particular, Moss (1963) found that in modern humans a robust and pneumatized crista galli is associated with sharp medial orbital margins, narrow (thus “closed”, sensu Moss) cribriform area, and thickened orbital roofs. He hypothesized that tension at the temporal pyramids could involve mechanical stress on the frontal anchorage of the falx cerebri via the tentorial structures. Usually, the cells of the crista are derived from the development of the frontal sinus (Shapiro and Janzen, 1960), and the tomographic sections of SCP1 show they have a direct communication with the ethmoidal air cells. The tilted morphology of the crista in some robust Middle Pleistocene specimens was hypothesized to be related to the backward shifting of the frontal lobes relative to the orbital roof (Seidler et al., 1997). Conversely, while in SCP1 the crista is tilted and pneumatized, the frontal lobes are not displaced posteriorly, requiring a different explanation. Unfortunately for comparative purposes, our present knowledge of the functional and structural morphology of the crista galli is very poor. No differences from the modern morphology have been described in the Middle Pleistocene sample from Sima de los Huesos (Arsuaga et al., 1997). The late archaic *Homo* endocast from Eliye Springs shows a pneumatized but not tilted crista, which does not contact the frontal boundary of the anterior fossa (Brauer et al., 2004). The isolated crista galli Krapina 44 does not show a pattern comparable to the morphology of SCP1 (Radović et al., 1988; Kricun et al., 1999). Thus, the latter cannot be considered representative of the pre-Würmian European populations for this feature.

Concerning the large right clinoid process and the left sella bridge, it is important to note that the digital resolution of the fossil matrix around the clivus is not complete enough to ensure that the morphological details are not being confused with geological inclusions. In general, the prevalence of sella bridges is quite heterogeneous in modern human populations, more frequent in males and on the left side, not dependent upon age, and interesting because of its probable heritability (see Hauser and De Stefano, 1989).

A final remark concerns SCP1's platycephaly. Considering the major endocranial axis from the frontal to the occipital poles, and taking into account the mentioned allometric vertical heightening of the vault, it seems that such platycephaly is related to a vertical flattening of the lower (temporo cerebellar)

areas, more than to a limited extension of the vault itself. Interestingly, SCP1 displays a very flexed cranial base (Sergi, 1944). Considering the importance of the basicranial angle in overall cranial architecture (Ross and Henneberg, 1995; McCarthy, 2001), the interesting morphology of the crista galli, and the allometric component of the endocranial functional matrix (Moss and Young, 1960), future research should aim to provide some structural hypotheses for this anatomical network, once the available data exists to support more robust statistical approaches.

Conclusions

Although the main endocranial diameters of SCP1 approach the values found in less encephalized morphotypes (i.e., *Homo erectus*) and, similarly, the middle meningeal vascular system shows a more developed posterior network, the information on cerebral shape and proportions supports the interpretation of this fossil cranium as a definite Neandertal specimen. In particular, the lateral development of the frontal lobes and the morphology of the parietal areas suggest a derived Neandertal brain structure, generally described in La Chapelle-aux-Saints and La Ferrassie as “long, low, and broad” (Holloway et al., 2004).

The accretion model (e.g., Dean et al., 1998; Hublin, 2000) proposes one single evolutionary lineage for the European populations during the mid-to-late Pleistocene, independently from the recognition of sequential stages (chronospecies). Nevertheless, the European fossil record between Middle and Late Pleistocene hardly supports the evidence of a linear and gradual process of change (e.g., Tattersall and Schwartz, 2006). Some endocranial metric variations fail to demonstrate discrete steps along the hypothesized anagenetic process (Bruner et al., 2006). On the other hand, when the distinction between *Homo heidelbergensis* and *Homo neanderthalensis* is considered, these results support the inclusion of SCP1 within the second group, despite its small cranial size and pre-Würmian chronology. This conclusion is consistent with analyses previously carried out on both the Saccopastore specimens, as far as the ectocranial morphology (e.g., Sergi, 1944, 1948), discrete traits (Condemi, 1992; Manzi et al., 1996), or skull shape (e.g., Bruner et al., 2004) are concerned.

Even in their earliest representatives, Neandertals seem to be characterized by a well-defined brain morphology. Such a combination of derived and plesiomorphic traits further emphasizes the phylogenetic independence of the extinct species *Homo neanderthalensis*, as already supported by a number of different biological perspectives (e.g., Manzi et al., 2000a,b; Ponce de León and Zollikofer, 2001; Lieberman et al., 2002; Harvati et al., 2004; Ramirez Rozzi and Bermudez de Castro, 2004; Serre et al., 2004; Rosas et al., 2006).

Acknowledgements

The CT-scan of Saccopastore 1 was performed at the Clinica Pio XI (Roma) and the stereolithography of the endocast was modelled by the Materialise Company (Leuven,

Belgium). Endocranial comparative data were collected at the Museum of Anthropology “Giuseppe Sergi” (Dipartimento di Biologia Animale e dell’Uomo, University La Sapienza, Roma), at the Istituto Italiano di Paleontologia Umana (IsIPU, Roma), and at the Institute de Paléontologie Humaine (IPH, Paris). We are grateful to Juan Luis Arsuaga, Henry and Marie-Antoinette de Lumley, Dominique Grimaud-Hervé, Gianfranco Gualdi, Pietro Passarello, Aldo and Eugenia Segre, Dennis Slice, and Christoph Zollikofer for their help, encouragement, and suggestions. The editors and two anonymous reviewers provided very useful comments on an earlier version of this manuscript. This work has been supported by the Italian Ministry for the University and Research (including Cofin/PRIN grants).

Appendix. Supplementary material

Supplementary data associated with this article can be found in the online version at doi: [10.1016/j.jhevol.2007.08.014](https://doi.org/10.1016/j.jhevol.2007.08.014)

References

- Arsuaga, J.L., Martínez, I., Gracia, A., Lorenzo, C., 1997. The Sima de los Huesos crania (Sierra de Atapuerca, Spain). A comparative study. *J. Hum. Evol.* 33, 219–281.
- Begun, D., Walker, A., 1993. The endocast. In: Walker, A., Leakey, R. (Eds.), *The Nariokotome Homo erectus Skeleton*. Springer-Verlag, Berlin, pp. 326–358.
- Bookstein, F.L., 1989. Principal warps: thin-plate spline and the decomposition of deformations. *IEEE Trans. Pattern Anal. Mach. Intell.* 11, 567–585.
- Bookstein, F.L., 1991. *Morphometric Tools for Landmark Data*. Cambridge University Press, Cambridge.
- Bradshaw, J.L., 1988. The evolution of human lateral asymmetry: new evidence and second thoughts. *J. Hum. Evol.* 17, 615–637.
- Brauer, G., Groden, C., Groning, F., Kroll, A., Kupczik, K., Mbu, E., Pommert, A., Schiemann, T., 2004. Virtual study of the endocranial morphology of the matrix-filled cranium from Eliye Springs, Kenya. *Anat. Rec. A* 276, 113–133.
- Breuil, H., Blanc, A.C., 1936. Le nouveau crane de Saccopastore, Rome. *L’Anthropologie* 46, 1–16.
- Bruner, E., 2003a. Fossil traces of the human thought: paleoneurology and the evolution of the genus *Homo*. *Riv. Antropol.* 81, 29–56.
- Bruner, E., 2003b. Computer tomography and paleoneurology: the Saccopastore Neandertals and brain evolution in the European middle Pleistocene. Ph.D. Dissertation, University La Sapienza, Roma.
- Bruner, E., 2004. Geometric morphometrics and paleoneurology: brain shape evolution in the genus *Homo*. *J. Hum. Evol.* 47, 279–303.
- Bruner, E., 2006. From Verheyen to Bookstein: history of colobids and superimpositions. *J. Anthropol. Sci.* 84, 147–160.
- Bruner, E., Averini, M., Manzi, G., 2003b. Endocranial traits. Prevalence and distribution in a recent human population. *Eur. J. Anat.* 7, 23–33.
- Bruner, E., Mantini, S., Perna, A., Maffei, C., Manzi, G., 2005. Shape analysis of the middle meningeal vessels in *Homo erectus*, Neandertals, and modern humans. *Eur. J. Morphol.* 42, 217–224.
- Bruner, E., Manzi, G., 2005. CT-based description and phyletic evaluation of the archaic human calvarium from Ceprano, Italy. *Anat. Rec.* 285A, 643–658.
- Bruner, E., Manzi, G., 2006. Saccopastore 1: the earliest Neandertal? A new look at an old cranium. In: Harvati, K., Harrison, T. (Eds.), *Neandertals Revisited: New Approaches and Perspectives*. Springer, New York, pp. 23–36.
- Bruner, E., Manzi, G., Arsuaga, J.L., 2003a. Encephalization and allometric trajectories in the genus *Homo*: evidence from the Neandertal and modern lineages. *Proc. Natl. Acad. Sci. U.S.A.* 100, 15335–15340.
- Bruner, E., Manzi, G., Holloway, R., 2006. Krapina and Saccopastore: endocranial morphology in the pre-Würmian Europeans. *Period. Biol.* 108, 433–441.
- Bruner, E., Manzi, G., Passarello, P., 2002. The “Virtual” endocast of Saccopastore 1. General morphology and preliminary comparisons by geometric morphometrics. In: Mafart, B., Delingette, H. (Eds.), *Three-Dimensional Imaging in Paleoanthropology and Prehistoric Archaeology*, British Archeol. Records IS 1049. Archeopress, Oxford, pp. 17–24.
- Bruner, E., Saracino, B., Passarello, P., Ricci, F., Tafuri, M., Manzi, G., 2004. Midsagittal cranial shape variation in the genus *Homo* by geometric morphometrics. *Coll. Antropol.* 28, 99–112.
- Condemi, S., 1992. *Les Hommes Fossiles de Saccopastore et leur Relations Phylogénétiques*. CNRS, Paris.
- Dean, D., Hublin, J.J., Holloway, R., Ziegler, R., 1998. On the phylogenetic position of the pre-Neandertal specimen from Reilingen, Germany. *J. Hum. Evol.* 34, 485–508.
- Falk, D., 1987. Hominid paleoneurology. *Annu. Rev. Anthropol.* 16, 13–30.
- Falk, D., 1993. Meningeal arterial patterns in great apes: implications for hominid vascular evolution. *Am. J. Phys. Anthropol.* 92, 81–97.
- Falk, D., Nicholls, P., 1992. Meningeal arteries in rhesus macaques (*Macaca mulatta*): implications for vascular evolution in anthropoids. *Am. J. Phys. Anthropol.* 89, 299–308.
- Galaburda, A.M., LeMay, M., Kemper, T.L., Geschwind, N., 1978. Right-left asymmetries in the brain. *Science* 199, 852–856.
- Gracia, A., 1991. Impresiones endocraneales del hombre de Ibeas. In: Rebas, E., Calderón, R. (Eds.), *VI Congreso de Antropología*. Universidad del País Vasco, Bilbao, pp. 351–360.
- Grimaud-Hervé, D., 1997. *L’évolution de l’enchéphale chez Homo erectus et Homo sapiens*. CNRS Editions, Paris.
- Hammer, Ø., Harper, D.A.T., Ryan, P.D., 2001. PAST: Paleontological statistics software package for education and data analysis. *Palaeontol. Electronica* 4, 1–9.
- Harvati, K., Frost, S.R., McNulty, K.P., 2004. Neandertal taxonomy reconsidered: Implications of 3D primate models of intra- and interspecific differences. *Proc. Natl. Acad. Sci. U.S.A.* 101, 1147–1152.
- Hauser, G., De Stefano, G.F., 1989. *Epigenetic Variants of the Human Skull*. Schweizerbart, Stuttgart.
- Hellige, J.B., 1993. *Hemispheric asymmetry*. Harvard University Press, Cambridge.
- Hjalgrim, H., Lynnerup, N., Liversage, M., Rosenklint, A., 1995. Stereolithography: potential applications in anthropological studies. *Am. J. Phys. Anthropol.* 97, 329–333.
- Holloway, R.L., 1978. The relevance of endocasts for studying primate brain evolution. In: Noback, C.R. (Ed.), *Sensory Systems of Primates*. Plenum Press, New York, pp. 181–200.
- Holloway, R.L., 1980. Indonesian “Solo” (Ngandong) endocranial reconstructions: some preliminary observations and comparisons with Neandertal and *Homo erectus* group. *Am. J. Phys. Anthropol.* 553, 285–295.
- Holloway, R.L., 1981. Volumetric and asymmetry determinations on recent hominid endocasts: Spy I and Spy II, Djebel Ihroud I, and the Salé *Homo erectus* specimen. With some notes on Neandertal brain size. *Am. J. Phys. Anthropol.* 55, 385–393.
- Holloway, R.L., Broadfield, D.C., Yuan, M.S., 2004. Brain endocasts: The paleoneurological evidence. In: *The Human fossil record, vol. III*. Wiley-Liss, Hoboken, New Jersey.
- Holloway, R.L., De La Costelareymondie, M.C., 1982. Brain endocast asymmetry in pongids and hominids: some preliminary findings on the paleontology of cerebral dominance. *Am. J. Phys. Anthropol.* 58, 101–110.
- Hublin, J.J., 2000. Modern-nonmodern hominid interactions: A Mediterranean perspective. In: Bar-Yosef, O., Pilbeam, D. (Eds.), *The Geography of Neandertals and Modern Humans in Europe and the Great Mediterranean*. Peabody Museum Bulletin, 8. Harvard University, Cambridge, pp. 157–182.
- Kimbel, W.H., 1984. Variation in the pattern of cranial venous sinuses and hominid phylogeny. *Am. J. Phys. Anthropol.* 63, 243–263.
- Kricun, M., Monge, J., Mann, A., Finkel, G., Lampl, M., Radović, J., 1999. The Krapina hominids. A radiographic atlas of the skeletal collection.

- Croatian Natural History Museum, Zagreb.
- Le May, M., 1976. Morphological cerebral asymmetries of modern man, fossil man, and nonhuman primates. *Ann. N. Y. Acad. Sci.* 280, 349–366.
- Lieberman, D.E., Mc Bratney, B.M., Krovitz, G., 2002. The evolution and development of cranial form in *Homo sapiens*. *Proc. Natl. Acad. Sci. U.S.A.* 99, 1134–1139.
- Manzi, G., 2004. Human evolution at the Matuyama-Brunhes boundary. *Evol. Anthropol.* 13, 11–24.
- Manzi, G., Bruner, E., Caprasecca, S., Gualdi, G., Passarello, P., 2001. CT-scanning and virtual reproduction of the Saccopastore Neandertal crania. *Riv. Antropol.* 79, 61–72.
- Manzi, G., Gracia, A., Arsuaga, J.L., 2000b. Cranial discrete traits in the Middle Pleistocene humans from Sima de los Huesos (Sierra de Atapuerca, Spain). Does hypostosis represent any increase in “ontogenetic stress” along the Neandertal lineage? *J. Hum. Evol.* 38, 425–446.
- Manzi, G., Passarello, P., 1991. Antènèandertaliens et Nèandertaliens du Latium (Italie Centrale). *L’Anthropologie* 95, 501–522.
- Manzi, G., Saracino, B., Bruner, E., Passarello, P., 2000a. Geometric morphometric analysis of mid-sagittal cranial profiles in Neandertals, modern humans, and their ancestors. *Riv. Antropol.* 78, 193–204.
- Manzi, G., Vienna, A., Hauser, G., 1996. Developmental stress and cranial hypostosis by epigenetic trait occurrence and distribution: an exploratory study on the Italian Neandertals. *J. Hum. Evol.* 30, 511–527.
- Marcocci, V., 1942. L’arteria meningea media negli uomini recenti, nel sinantropo e nelle scimmie. *Riv. Antropol.* 34, 407–436.
- McCarthy, R.C., 2001. Anthropoid cranial base architecture and scaling relationships. *J. Hum. Evol.* 40, 41–66.
- Moss, M.L., 1963. Morphological variations of the crista galli and medial orbital margin. *Am. J. Phys. Anthropol.* 21, 159–164.
- Moss, M.L., Young, R.W., 1960. A functional approach to craniology. *Am. J. Phys. Anthropol.* 18, 281–292.
- O’Laughlin, V., 1996. Comparative endocranial vascular changes due to craniosynostosis and artificial cranial deformation. *Am. J. Phys. Anthropol.* 101, 369–385.
- Radović, J., Smith, F.H., Trinkaus, E., Wolpoff, M.H., 1988. The Krapina Hominids. Croatian National History Museum, Zagreb.
- Ramirez Rozzi, F.V., Bermudez de Castro, J.M., 2004. Surprisingly rapid growth in Neandertals. *Nature* 428, 936–939.
- Recheis, W., Weber, G.W., Schafer, K., Prossinger, H., Knapp, R., Seidler, H., zur Nedden, D., 1999. New methods and techniques in anthropology. *Coll. Antropol.* 23, 495–509.
- Rightmire, G.P., 1990. *The Evolution of Homo erectus. Comparative Anatomical Studies of an Extinct Human Species.* Cambridge University Press, Cambridge.
- Rosas, A., Bastir, M., Martinez-Maza, C., Garcia Taberero, A., Lalueza Fox, C., 2006. Inquiries into Neandertal craniofacial development and evolution: “accretion” versus “organismic” models. In: Harvati, K., Harrison, T. (Eds.), *Neandertals Revisited: New Approaches and Perspectives.* Springer, New York, pp. 37–70.
- Ross, C., Henneberg, M., 1995. Basicranial flexion, relative brain size, and facial kyphosis in *Homo sapiens* and some fossil hominids. *Am. J. Phys. Anthropol.* 98, 575–593.
- Saban, R., 1979. Le système veineux méningé de l’homme fossile de Biache-Saint-Vaast Pas de Calais, d’après le moulage endocranien. *C.R. Acad. Sci. Paris D289*, 1129–1132.
- Saban, R., 1982. Le système des veines méningées moyennes chez les hommes fossiles de Tchécoslovaquie, d’après le moulage endocranien. *Anthropos* 21, 281–295.
- Saban, R., 1995. Image of the human fossil brain: endocranial casts and meningeal vessels in young and adult subjects. In: Changeaux, P., Chavaillon, J. (Eds.), *Origins of the Human Brain.* Clarendon Press, Oxford, pp. 11–38.
- Schoenemann, P.H., Gee, J., Avants, B., Holloway, R.L., Monge, J., Lewis, J., 2006. Validation of plaster endocast morphology through 3D CT image analysis. *Am. J. Phys. Anthropol.* 132, 183–192.
- Seidler, H., Falk, D., Stringer, C., Wilfing, H., Muller, G.B., zur Nedden, D., Weber, G.W., Recheis, W., Arsuaga, J.L., 1997. A comparative study of stereolithographically modelled skulls of Petralona and Broken Hill: implications for future studies of Middle Pleistocene hominid evolution. *J. Hum. Evol.* 33, 691–703.
- Sergi, S., 1929. La scoperta di un cranio del tipo di Neandertal presso Roma. *Riv. Antropol.* 28, 457–462.
- Sergi, S., 1944. Craniometria e craniografia del primo paleantropo di Saccopastore. *Ric. Morfol.* 20–21, 733–791.
- Sergi, S., 1948. L’uomo di Saccopastore. *Paleontogr. Italica XLII*, 25–164.
- Sergi, S., 1962. The Neandertal Palaeanthropi in Italy. In: Howells, W.W. (Ed.), *Ideas on Human Evolution. Selected Essays, 1949–1961.* Harvard University Press, Cambridge, pp. 500–506.
- Serre, D., Langaney, A., Chech, M., Teschler-Nicola, M., Paunovic, M., Mennecier, P., Hofreiter, M., Possnert, G., Paabo, S., 2004. No evidence of Neandertal mtDNA contribution to early modern humans. *PLoS Biol.* 2, 313–317.
- Shapiro, R., Janzen, A.H., 1960. *The Normal Skull.* P.B. Hoeber, Inc., New York.
- Slice, D.E., 2000. *Morpheus et al. Ecology and Evolution.* SUNY at Stony Brook, NY.
- Spoor, F., Jeffery, N., Zonneveld, F., 2000. Using diagnostic radiology in human evolutionary studies. *J. Anat.* 197, 61–76.
- StatSoft, 1995. *Statistica 5.1. Data analysis software.* StatSoft Inc.
- Stringer, C.B., Hublin, J.J., Vandermeersch, B., 1984. The origin of anatomically modern humans in Western Europe. In: Smith, F., Spencer, F. (Eds.), *The Origins of Modern Humans. A World Survey of the Fossil Evidence.* A.R. Liss, New York, pp. 51–135.
- Tattersall, I., Schwartz, J.H., 2006. The distinctiveness and systematic context of *Homo neanderthalensis*. In: Harvati, K., Harrison, T. (Eds.), *Neandertals Revisited: New Approaches and Perspectives.* Springer, New York, pp. 9–22.
- Wu, X., Schepartz, L.A., Falk, D., Liu, W., 2006. Endocranial cast of Hexian *Homo erectus* from South China. *Am. J. Phys. Anthropol.* 130, 445–454.
- Zelditch, M.L., Swidersky, D.L., Sheets, H.D., Fink, W.L., 2004. *Geometric Morphometrics for Biologists.* Elsevier, San Diego.
- Zollikofer, C.P.E., Ponce de León, M.S., Martin, R.D., 1998. Computer assisted paleoanthropology. *Evol. Anthropol.* 6, 41–54.